PROTEINS: Structure, Function, and Genetics 24:73–80 (1996)

Crystal Structure of the *Trypanosoma cruzi* Trypanothione Reductase·Mepacrine Complex

Elke M. Jacoby,[1,2] Ilme Schlichting,[2,3] Christina B. Lantwin,[2] Wolfgang Kabsch,[2] and R. Luise Krauth-Siegel[1]

[1]Institut für Biochemie II, Universität Heidelberg, D-69120 Heidelberg, Germany; [2]Max-Planck-Institut für Medizinische Forschung, Abteilung Biophysik, D-69120 Heidelberg, Germany; and [3]Max-Planck-Institut für Molekulare Physiologie, Abteilung Physikalische Biochemie, D-44139 Dortmund, Germany

ABSTRACT **The three-dimensional structure of the complex between *Trypanosoma cruzi* trypanothione reductase (TR) (EC 1.6.4.8) and the antiparasitic drug mepacrine (quinacrine) has been solved at 2.9 Å resolution. Mepacrine is a competitive inhibitor of TR but does not affect human glutathione reductase (GR), a closely related host enzyme. Of particular importance for inhibitor binding are four amino acid residues in the disulfide substrate-binding site of TR that are not conserved in human GR, namely, Glu-18 (Ala-34 in GR), Trp-21 (Arg-37), Ser-109 (Ile-113), and Met-113 (Asn-117).**

The acridine ring of mepacrine is fixed at the active site close to the hydrophobic wall formed by Trp-21 and Met-113. Specific pairwise interactions between functional groups of the drug and amino acid side chains include the ring nitrogen and Met-113, the chlorine atom and Trp-21, and the oxymethyl group and Ser-109. The alkylamino chain of mepacrine points into the inner region of the active site and is held in position by a solvent-mediated hydrogen bond to Glu-18.

The structure of the complex shows for the first time the atomic interactions between TR and an inhibitory ligand. This is a crucial step towards the rational design of inhibitors that might be suited as drugs against Chagas' disease. © 1996 Wiley-Liss, Inc.

Key words: X-ray crystallography, flavoenzyme, drug target, *Trypanosoma cruzi*

INTRODUCTION

Parasitic protozoa of the order Kinetoplastida are the causative agents of tropical diseases such as African sleeping sickness, Nagana cattle disease, Chagas' disease, Kala-azar, and Oriental sore. Besides other metabolic peculiarities, these protozoa possess a unique thiol metabolism.[1] In contrast to nearly all eucaryotes and procaryotes, they lack the enzyme GR but have a TR instead.[2,3] The enzyme keeps the main thiols of the parasite, namely, monoglutathionylspermidine and bis(glutathionyl)spermidine [trypanothione, $T(SH)_2$][4] in the reduced state:

$$TS_2 + NADPH + H^+ \rightleftharpoons T(SH)_2 + NADP^+$$

TR of *Trypanosoma cruzi*, the causative agent of Chagas' disease, was purified from epimastigote parasites,[5] and the gene was cloned and overexpressed in *E. coli*.[6] The three-dimensional structures of TR from *Crithidia fasciculata*[7,8] and from *T. cruzi*[9] were solved. The enzyme is an FAD-cystine-oxidoreductase as are GR, lipoamide dehydrogenase, and mercuric ion reductase.[10] *T. cruzi* TR shares many physical and chemical properties with human GR—the closest related host enzyme—except their mutually exclusive specificity toward their disulfide substrates.[5]

The sensitivity of *T. cruzi* against oxidative stress, together with the fact that its defense mechanisms rely on the trypanothione system, make TR an attractive target molecule for drug design against Chagas' disease. Kinetic studies in solution revealed different types of compounds as inhibitors.[3,11] The cytostatic agent BCNU covalently modifies reduced TR. Most probably BCNU carbamoylates one of the active-site cysteines in the reduced enzyme species.[12] Nitrofuran and naphthoquinone derivatives can be turncoat inhibitors of TR.[12–14] Another type of inhibitors is represented by tricyclic ring structures that act as competitive ligands versus trypanothione disulfide. Examples are mepacrine (Fig. 1), an acridine derivative,[15] and phenothiazines and benzacepines.[16] None of these compounds interferes with GR. The interactions between *C. fasciculata* TR and the benzacepine clomipramine were studied by

Abbreviations: TR, trypanothione reductase (EC 1.6.4.8); GR, glutathione reductase (EC 1.6.4.2); $T(SH)_2$, reduced trypanothione [N^1N^8-bis(glutathionyl)spermidine]; TS_2, trypanothione disulfide; rms, root mean square; 1 Å = 0.1 nm; Tris, tris(hydroxymethyl)aminomethane; BCNU, carmustine,1,3-bis(2-chloroethyl)-1-nitrosourea; DMSO, dimethylsulfoxide; residues with primed numbers belong to the other subunit.

Received May 19, 1995; revision accepted August 14, 1995.

Address reprint requests to R. Luise Krauth-Siegel, Institut für Biochemie II, Im Neuenheimer Feld 328, D-69120 Heidelberg, Germany.

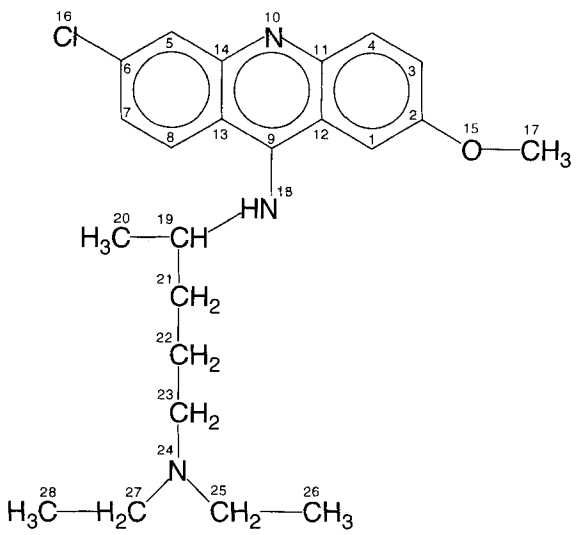

Fig. 1. Structure of mepacrine. The numbering corresponds to that used in the structure of free mepacrine.[22]

molecular modeling,[16] but no three-dimensional structure of a TR·inhibitor complex has been solved so far.

For the rational development of a specific inhibitor of TR the structures of several enzyme·inhibitor complexes should be known in atomic detail. Understanding the interactions between protein and ligands is fundamental for the synthesis of more specific inhibitors. Here we describe the three-dimensional structure of the complex between *T. cruzi* TR and the antiparasitic drug mepacrine (quinacrine).[17] Results obtained from kinetic studies with other acridine derivatives are discussed in light of the TR·mepacrine structure.

MATERIALS AND METHODS

Crystallographic Methods

Crystal preparation and data collection

Recombinant *T. cruzi* TR was purified and crystallized as described.[18] Crystals of the enzyme were grown by the hanging drop procedure. The protein solution (15 mg/ml) containing 500 mM sodium citrate and 2% octanoyl-N-methylglucamide in 50 mM sodium phosphate, 1 mM EDTA, pH 8.0, was allowed to equilibrate with 1.2 M sodium citrate at 20°C. The monoclinic crystals belonging to space group $P2_1$ (a = 136.79 Å, b = 91.15 Å, c = 126.64 Å, β = 94.01°) contain two dimers of the enzyme in the asymmetric unit.

For generating the enzyme·inhibitor complex, TR crystals were soaked in a solution containing mepacrine. Several conditions were tested that differed both in soaking time (1–7 days) and mepacrine concentration (50 μM to saturated). The condition that resulted in additional electron density compared with the native enzyme was obtained by soaking crystals for 2 days at 20°C in a saturated solution of mepacrine in 1.4 M sodium citrate, 20 mM Tris, 1 mM EDTA, pH 8.0. During that time, the crystal (1,000 × 250 × 250 μm^3) did not undergo any structural changes as judged by light microscopy. The crystal was mounted using the soaking solution.

Diffraction data were collected at 4°C at station X11 of the DESY Synchrotron (Hamburg) using a MAR image plate and a wavelength of 0.93 Å. Intensities were measured in 1° frames with exposure times of 60 s/frame and processed by the program XDS.[19,20]

The data consist of 220,206 reflections, 62,269 of which are unique, corresponding to a completeness of 89.9% at a resolution of 2.9 Å. The statistics of the data set are shown in Table I.

Refinement procedure

Since the soaked crystals were isomorphous with those of the native enzyme, the refined structure at 3.3 Å[9] served as a starting model for the refinement performed with X-PLOR[21] using the standard protocol for conjugate-gradient minimization and slow cooling. The first round of refinement was carried out by imposing non-crystallographic symmetry between the two TR dimers in the asymmetric unit without any inhibitor coordinates. No restraints were applied for residues in an 8 Å sphere centered at Tyr-110 (the expected binding site as inferred from kinetic data) to allow for any structural changes due to binding of the inhibitor.

$(2F_{obs} - F_{calc})$ exp $i\alpha_{calc}$ electron density maps revealed high electron density in only one active site of one dimer (no other continuous planar density large enough for the tricyclus was found after careful inspection of the map). To account for this inequality, refinement was continued with the four TR monomers of the asymmetric unit. Again, non-crystallographic symmetry restraints were imposed on the structure except for the four active sites, and no inhibitor molecule was included. After another round of simulated annealing refinement, a $2F_{obs} - F_{calc}$ electron density map was calculated that again showed unaccounted electron density at the expected mepacrine binding site in one of the four active sites. This result was confirmed by a difference Fourier map, as shown in Fig. 2A.

For further refinement we used a model of mepacrine (Fig. 1) with the coordinates given in the crystal structure of the free compound.[22] Mepacrine was built into its presumed electron density using the interactive graphics program FRODO,[23] adapted to an Iris 4GT Silicon Graphics (Mountain View, CA) by C.M. Cambillau. Since high electron density was found only for the aromatic ring system, the fit of the acridine moiety to the density was optimized. Several orientations of the inhibitor molecule were refined, but only one resulted in a significantly improved electron density map. This map revealed ad-

TABLE I. Statistics of Crystallographic Data

		Resolution shells			
Mepacrine-soaked crystal	Overall	∞–10.0	10.0–6.0	6.0–4.0	4.0–2.9
No. of measured reflections	220,206	4,675	24,821	69,136	121,574
No. of unique reflections	62,269	1,483	5,740	16,955	38,091
R* (%)	7.0	3.8	5.1	5.9	15.2
Completeness of all the data (%)	89.9	83.1	92.2	91.1	89.3
Data with $I/\sigma > 1$	82.2	82.5	91.5	90.0	77.4
Data with $I/\sigma > 3$	74.9	81.8	89.5	87.7	66.9
R† (%) using data with $I/\sigma > 1$	22.4				
R_{free}† (%) using data with $I/\sigma > 1$	27.7				

*$\Sigma_h\Sigma_i|I_{hi} - I_h|/\Sigma_{hi}I_{hi}$ where h are unique reflection indices and I_{hi} are the intensities of symmetry equivalent reflections giving a mean value of I_h.
†$\Sigma||F_{obs}| - |F_{calc}||/\Sigma|F_{obs}|$ where F_{obs} and F_{calc} are observed and model structure factor amplitudes, respectively. For the calculation of R_{free} 10% of the reflections were used. No bulk solvent correction was applied to the data.

ditional density for the alkylamino side chain and the chlorine atom, thus defining the orientation of mepacrine unambiguously (Fig. 2B).

To verify the presence of the single inhibitor molecule per asymmetric unit, we used an approach reminiscent of heavy atom refinement procedures where occupancy and temperature factors of putative derivative sites are refined separately even at low resolution and where this information is used to confirm or discard possible heavy atom binding sites. Thus, mepacrine coordinates were included in each active site of the two TR dimers. Setting the temperature factor to 30 Å^2, the mepacrine occupancies and the temperature factors were refined. Even though occupancy and temperature factors are highly correlated, and the individual values are not very accurate at a resolution of 2.9 Å, the pair of occupancy and temperature factors describes one possible interpretation of the data. As expected from the electron density map, the occupancy of three mepacrine molecules converged to zero, whereas that of the fourth converged to 0.3 with a temperature factor of 70 Å^2. The occupancy of mepacrine was fixed at 0.3 in the next round of refinement, which included four TR and FAD molecules and one mepacrine. The final structure refinement included rigid body refinement of the single mepacrine molecule coupled with separate occupancy and temperature factor refinement and resulted in a temperature factor of 30.7 Å^2. The estimated error of atomic positions as derived from a σ_A plot[24] is 0.27 Å. The final crystallographic R-factor is 22.4%, and the free R-factor is 27.7% for 56,961 reflections with $I/\sigma(I) > 1$ between 10.0 and 2.9 Å. The stereochemistry of the model is good, with deviations of 0.013 Å in bond lengths and 1.4° in angles.

Biochemical Methods

Materials

Mepacrine was provided by Rhône-Poulenc Rorer (Dagenham, Essex, UK). Acridine-9-carbonic acid, acridine-4,9-dicarbonic acid, 9-aminoacridine, and acridine were obtained from Sigma (Germany). Trypanothione (TS_2) was purchased from Bachem (Switzerland). All other reagents (from Boehringer, Merck, Roth, and Sigma) were of the highest available purity.

TR assay

TR activity was measured at 25°C in a 150-20 Hitachi Spectrophotometer (Colora Germany). The standard assay (1 ml) contained 100 μM NADPH, 120 μM trypanothione disulfide (TS_2), and 5–10 mU TR in TR assay buffer (40 mM Hepes, 1 mM EDTA, pH 7.5).[12] After starting the reaction by the addition of TS_2 the absorbance decrease at 340 nm was followed.

Inhibition of TR by acridines

Stock solutions (10 mM) of the poorly water soluble derivatives acridine-9-carbonic acid and acridine were prepared in DMSO. Mepacrine, acridine-4,9-dicarbonic acid, and 9-aminoacridine were directly dissolved in TR assay buffer. The concentration of DMSO in the reaction mixture never exceeded 10%, which has no influence on enzyme activity, as proved by control assays containing the same concentration of DMSO.

Inhibition constants were determined according either to Lineweaver-Burk at two different inhibitor concentrations or to Dixon at three substrate concentrations.

Spectroscopic Detection of mepacrine in the Soaked Crystal

To verify the presence of mepacrine in the TR crystal used for data collection, the crystal was dissolved in 50 μl TR assay buffer and the absorption spectrum recorded using microcuvettes with a total volume of 100 μl in a Beckmann DU-65 Spectrophotometer.

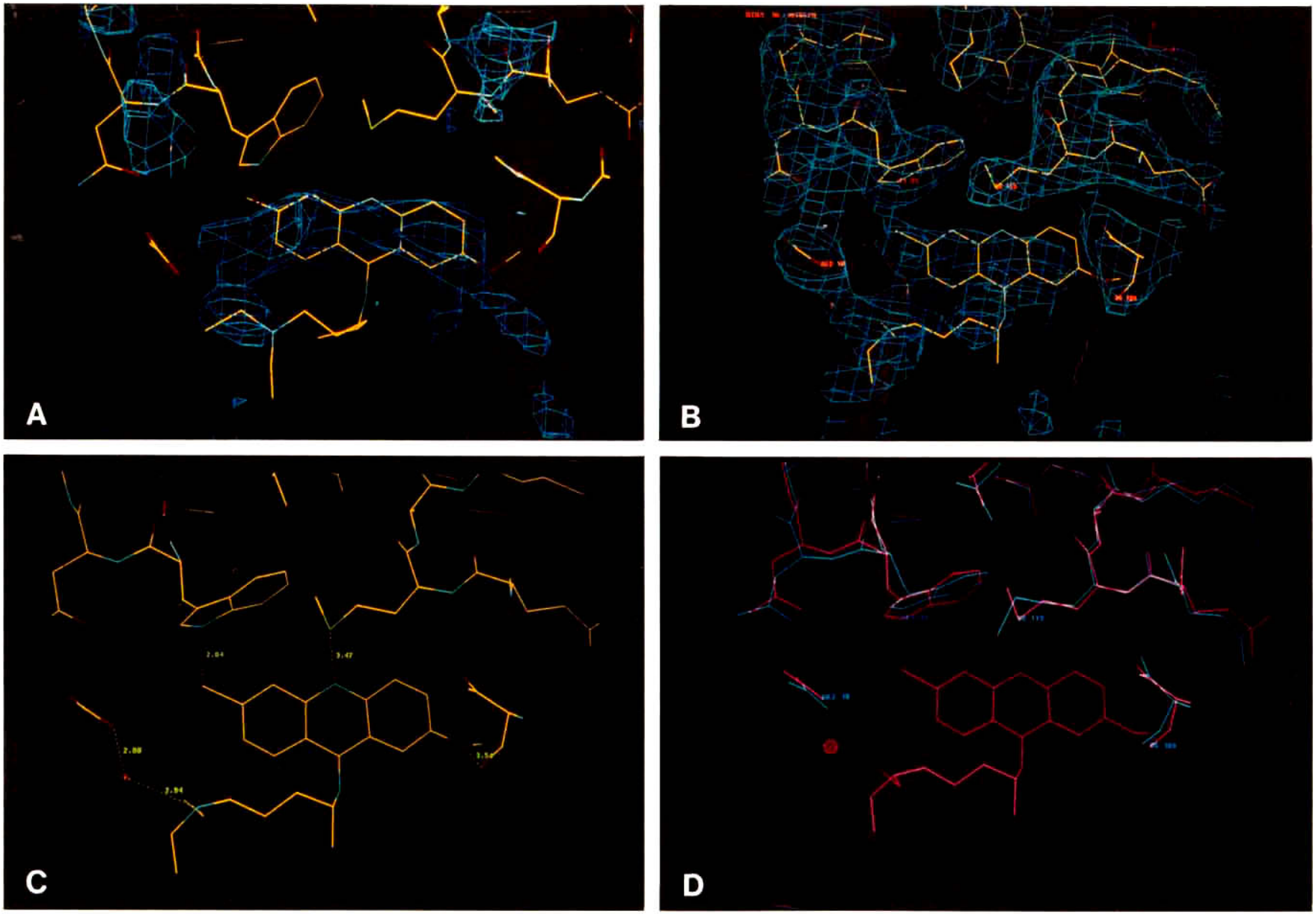
A
B
C
D

RESULTS AND DISCUSSION

Quality of the Refined Structure

The three-dimensional structure of the complex between mepacrine and *T. cruzi* TR was solved at 2.9 Å resolution by difference Fourier methods. The structure of the unliganded protein at 3.3 Å resolution[9] served as a starting model for the refinement, since the crystals of the enzyme·inhibitor complex were isomorphous with those of the native enzyme.[9]

Trypanothione reductase is a homodimer, each subunit consisting of 492 amino acid residues and one FAD molecule as a prosthetic group. The enzyme crystallizes with two dimers in the asymmetric unit. The final structural model consists of four protein monomers (residues 4–484 of each polypeptide chain) resulting in 14,808 non-hydrogen protein atoms and four FAD (212 atoms), one mepacrine (28 atoms), and two solvent molecules in one active site (WAT1 and WAT2). The three N-terminal and seven C-terminal residues of each subunit that have no well-defined electron density are not included in the model. The mean temperature factor is 21.6 $Å^2$ for all residues and 30.7 $Å^2$ for the mepacrine molecule. Since the completeness of our data ($I/\sigma > 1$) was 82.2%, we analyzed the influence of the missing data on the quality of the electron density map. For that purpose intensities were calculated from our final refined TR·mepacrine model only for the observed reflection indices. The $2F_{obs} - F_{calc}$ map of these calculated data agreed well with the map obtained from the observed data. The fit of the mepacrine molecule to the final electron density map is good, taking into account the resolution of 2.9 Å, the low occupancy, and the presence of only one inhibitor molecule per tetramer (Fig. 2B).

Binding of only one mepacrine molecule per protein tetramer is probably due to differences in the solvent accessibility of the protein subunits. At least for two monomers, binding of the inhibitor is most unlikely since symmetry-related molecules block the access to the active site. This observation corroborates the results of the occupancy and temperature factor refinement. Using a model of one mepacrine per TR monomer active site yielded a finite occupancy (0.3) for only one inhibitor molecule, which had a temperature factor of 70 $Å^2$. In the second refinement cycle with the tetramer, four FAD molecules, and *one* mepacrine molecule, the refined occupancy of 0.3 for the single inhibitor molecule was kept fixed and the temperature factor decreased to 54 $Å^2$. For optimizing the position of the mepacrine molecule, a rigid body refinement for the ligand, followed by occupancy and temperature factor refinement, was carried out. During this final refinement step, the average thermal parameter of mepacrine dropped to 30.7 $Å^2$.

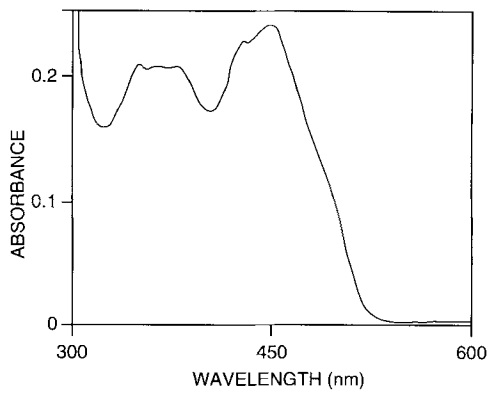

Fig. 3. Absorption spectrum of the trypanothione reductase·mepacrine complex. The TR crystal soaked with mepacrine, which was used for X-ray diffraction analysis, was dissolved in 50 µl 40 mM HEPES, 1 mM EDTA, pH 7.5, and the absorption spectrum was recorded. The spectrum obtained is the sum of the flavin and acridine absorptions. λ_{max} of the free enzyme is shifted from 461 nm to 450 nm for the complex. In addition, a small maximum arises at 344 nm due to the second absorption peak of mepacrine.

Binding of Mepacrine at the Active Site of TR

Mepacrine (quinacrine) was bound to *T. cruzi* TR by soaking a TR crystal in a saturated solution of the drug. The presence of the inhibitor in the crystal that had been subjected to X-ray data collection was confirmed by dissolving the crystal and recording the absorption spectrum (Fig. 3). The absorption maximum in the visible region of the flavoenzyme[5] at 461 nm is shifted to 450 nm, corresponding to the sum of FAD and acridine absorptions. The small peak arising at 344 nm is also caused by mepacrine.

TR is a homodimeric flavoenzyme. Both polypeptide chains are subdivided into four domains, namely, the FAD domain (residues 1–160), the NADPH domain (residues 161–290), the central domain (residues 291–360), and the interface domain (residues 361–492). The two identical active sites are formed by residues of both subunits. The peptide segments constructing the active site comprise residues 14–21, 52–58, 106–114, and 335–339 of one subunit and 396′–399′ and 461′–470′ of the other

Fig. 2. Binding of mepacrine to trypanothione reductase. **A:** Initial difference Fourier map calculated with coefficients ($F_{obs} - F_{calc}$) exp $i\alpha_{calc}$ that contained no coordinates for mepacrine. The contour level is 30% of the maximum density. No other continuous density large enough to fit the acridine ring was found in the map. **B:** The refined model of mepacrine together with the final $2F_{obs} - F_{calc}$ electron density. The contour level is at 15% of the maximum density. Included are the active site residues Glu-18, Trp-21, Ser-109, and Met-113, which are in direct contact with the inhibitor. **C:** Distances between mepacrine and active site residues. The direct contacts between the inhibitor and side chains of the protein are Cl16–Trp-21(NE1), 2.6 Å; N10–Met-113(SD), 3.5 Å, and O15–Ser-109(OG), 3.5 Å. N24 and Glu-18 form a solvent-mediated hydrogen bond, with N24–WAT2 (O) and WAT2 (O)–Glu-18 (OE2) distances of 2.9 Å and 2.6 Å, respectively. **D:** Structural changes of active site residues caused by the binding of mepacrine. The unliganded enzyme structure (light blue) is superimposed with that of the enzyme–inhibitor complex (light red). In the mepacrine·TR structure the S-CH_3 group of Met-113 is rotated by about 180° allowing the direct interaction with the ring nitrogen of the inhibitor.

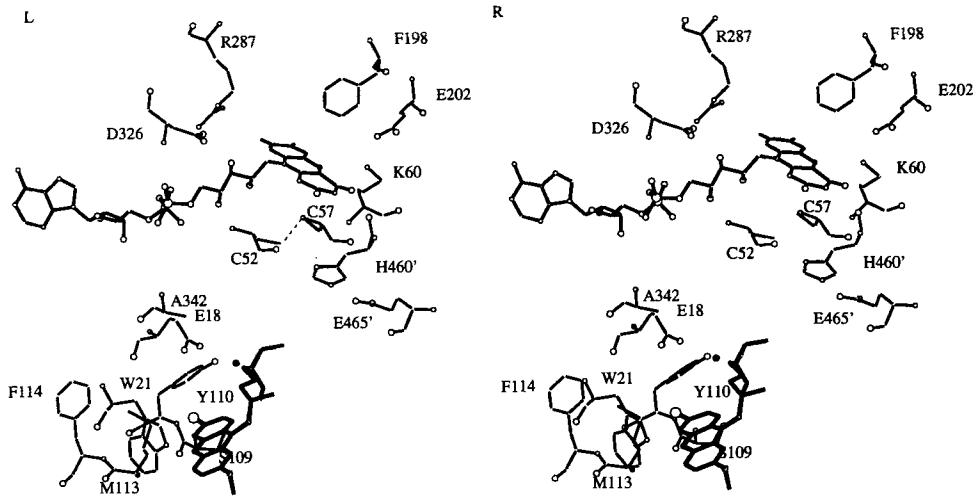

Fig. 4. Stereoplot of the active site of *T. cruzi* TR with bound mepacrine. The isoalloxazine ring of FAD forms the center of the active site. The dashed line represents the active site disulfide bridge. His-460′ and Glu-465′ are residues of the other subunit. Mepacrine (bold lines) binds to trypanothione reductase with the acridine ring close to the hydrophobic region formed by Trp-21 and Met-113, whereas the alkylamino chain is fixed to Glu-18 via a water molecule (black dot).

subunit. Of particular importance for substrate and (as shown here) also for inhibitor binding are five residues in the disulfide substrate binding site that are not conserved when comparing *T. cruzi* TR and human GR. These are Glu-18 (Ala-34 in GR), Trp-21 (Arg-37), Ser-109 (Ile-113),. Met-113 (Asn-117), and Ala-342 (Arg-347).[25] Trp-21 and Met-113 as well as Leu-17 and Phe-114 form a hydrophobic wall involved in substrate binding.[26]

Mepacrine is bound at the substrate-binding site of TR with the acridine ring close to Trp-21 and Met-113, whereas the N9-alkylamino chain points into the inner region of the active site toward Glu-18 (Fig. 4).

All substituents of the acridine ring are in contact with side chains of the protein (Fig. 2C). The methylether group at C2 of the acridine ring is in hydrogen bonding distance to the side chain oxygen of Ser-109 (Table II). The chlorine atom of mepacrine is close to the ring nitrogen of Trp-21 (Fig. 2). Obviously the halogen is stabilized by interacting with the positively polarized hydrogen of the indolyl nitrogen. The same type of interaction was described for the enzyme haloalkane dehalogenase complexed with the substrate 1,2-dichloroethane[27] where one chlorine atom of the substrate is fixed between the ring nitrogens of two Trp residues with Cl-N distances of 3.6 Å and 3.2 Å, respectively.

The ring nitrogen (N10) is 3.5 Å apart from the SD atom of Met-113. Since mepacrine is a weak base, a hydrogen bond between the protonated nitrogen and the sulfur atom may be formed. The observed distance falls into the range of 3.6 ± 0.3 Å of N-H·S hydrogen bonds in other proteins.[28,29] Although hydrogen bonds that involve a sulfur are not very com-

TABLE II. Residues of Trypanothione Reductase Surrounding the Bound Mepacrine in a 4 Å Sphere

Mepacrine atom acridine ring	Atom	(protein residue)	Distance (Å)
C2	CB	(Ser-109)	3.8
C2	O	(Ser-109)	3.5
C3	O	(Ser-109)	3.1
C3	CB	(Met-113)	3.9
C4	CB	(Met-113)	3.3
C4	CG	(Met-113)	3.7
C4	O	(Ser-109)	3.8
C5	CD2	(Trp-21)	3.7
C5	CE2	(Trp-21)	3.4
C5	NE1	(Trp-21)	3.6
C5	CZ2	(Trp-21)	3.6
C6	CE2	(Trp-21)	3.8
C6	CD1	(Trp-21)	3.8
C6	NE1	(Trp-21)	3.6
N10	CG	(Met-113)	3.7
N10	SD	(Met-113)	3.5
O15	CB	(Ser-109)	3.0
O15	OG	(Ser-109)	3.5
O15	O	(Ser-109)	3.7
Cl16	CB	(Trp-21)	4.0
Cl16	CG	(Trp-21)	3.1
Cl16	CD2	(Trp-21)	3.7
Cl16	CE2	(Trp-21)	3.4
Cl16	CD1	(Trp-21)	2.5
Cl16	NE1	(Trp-21)	2.6
C17	CB	(Ser-109)	3.9
N9-chain			
C19	OH	(Tyr-110)	3.6
C21	OH	(Tyr-110)	3.2
N24,WAT2	OE2	(Glu-18)	2.9 and 2.6
C27	CD1	(Ile-338)	3.6
C28	CD1	(Ile-338)	3.9

TABLE III. Acridine Derivatives as Inhibitors of *T. cruzi* Trypanothione Reductase*

Compound	K_i (μM)	Inhibition at [inhibitor (μM)/TS_2 (μM)] (%)
Mepacrine	25 (21)†	
Acridine		0 (250/69)
9-Aminoacridine	59	
Acridine-9-dicarbonic acid		0 (250/69)
Acridine-4,9-dicarbonic acid		0 (250/69)

*The kinetics were measured in TR-assay-buffer, pH 7.5, as described under Materials and Methods. If a compound was only a weak inhibitor of TR, detailed kinetics were not carried out and % inhibition at a fixed concentration of inhibitor and disulfide substrate is given. Mepacrine and 9-aminoacridine are competitive inhibitors versus trypanothione disulfide, as shown by Lineweaver-Burk or Dixon plots.
†Inhibitor constant obtained in 20 mM Tris, 1 mM EDTA, pH 8.0, containing 1.2 M sodium citrate.

mon in proteins,[30] this type of interaction may be important for ligand fixation in TR. Upon mepacrine binding, the S-methyl group of Met-113 turns around by about 180°, which allows a direct contact with the inhibitor (Fig. 2D). Met-113 is one of the unique residues in the active site of TR. The dual property of methionine—it is the most flexible hydrophobic residue *and* able to accept a hydrogen bond—renders it well suited for binding ligands. In the structure of the TR·substrate complex[26] Met-113 is in close contact with the methylene groups of the spermidine moiety and concomitantly accepts a hydrogen bond from the N8-amino group of glutathionylspermidine.

At C9 mepacrine possesses an 8 Å long alkylamino chain that is directed into the inner region of the active site. The tertiary amino group N24 is protonated (as deduced from the structural data of free mepacrine[22]) and may form a water-mediated hydrogen bond with the carboxylate of Glu-18 (Table II and Fig. 2C). A contribution of the alkylamino substituent to the binding strength of mepacrine in TR was expected because of its structural similarity with the natural polyamines.[15] The kinetic results obtained with other derivatives also confirm that acridines lacking a suitable side chain are weaker inhibitors of TR, or do not inhibit TR at all (Table III and unpublished results).

Specificity of Mepacrine as a TR Inhibitor

Despite the close similarity between TR and GR, the latter enzyme is not inhibited by mepacrine.[15] Striking structural differences are the narrower binding site for the disulfide substrate in GR and the occurrence of Ala-34, Arg-37, Ile-113, Asn-117, and Arg-347 in GR, as outlined above. The overall positive charge of the GSSG binding site obviously prevents binding of the cationic amphiphilic drug. The specificity of inhibition is not simply due to the presence of a tricyclic structure since riboflavin analogs are much better inhibitors of GR than of TR.[31] In this case the tricyclic ring systems are bound between the protein subunits in a cavity that is significantly smaller in TR than in GR.

Inhibition of TR by Other Acridine Derivatives

Several acridine derivatives were tested as inhibitors of *T. cruzi* trypanothione reductase (Table III).

Mepacrine inhibits *T. cruzi* TR with a K_i value of 25 μM.[15] The competitive type of inhibition and the K_i value remained unchanged in the presence of 1.2 M sodium citrate in the assay mixture, i.e., under the ionic strength conditions occurring in the protein crystal. This is not surprising as mostly hydrophobic interactions are responsible for mepacrine binding in TR.

Acridine is not an inhibitor of the enzyme, which underscores the role of the substituents of mepacrine for binding to TR. The lack of inhibition of TR by acridine-9-carbonic acid and acridine-4,9-dicarbonic acid was expected because of their net negative charge. 9-Aminoacridine inhibits TR but to a lesser extent than mepacrine. Since other substituents are missing, it cannot be ruled out that 9-aminoacridine is bound to TR in a completely different way. For instance, it may be turned around, allowing the 9-amino group to interact with Met-113.

CONCLUSIONS

A rational strategy for the treatment of parasitic diseases is the design of compounds that selectively inhibit enzymes that are pivotal for the survival of the parasite.[32] TR is particularly suited for this purpose since it serves as a key enzyme of the parasite's thiol metabolism and does not occur in the mammalian host.

The antiparasitic drug mepacrine is a competitive inhibitor of TR but does not affect human GR, which is the most closely related host enzyme.[15] The crystallographic analysis of the TR·mepacrine complex shows for the first time the interactions between an inhibitor and the parasite enzyme in atomic detail. The structure now forms the basis for tailoring new inhibitors of *T. cruzi* TR with the aim of obtaining more selective drugs against Chagas' disease.

ACKNOWLEDGMENTS

We thank Dr. Christopher Walsh for providing the *T. cruzi* TR clone. We also thank Klaus Scheffzek for fruitful discussions. This work was supported by the Deutsche Forschungsgemeinschaft (DFG Kr 1242/1-1) and the Bundesministerium für Forschung und Technik (BMFT-Schwerpunkt Tropical Medicine Heidelberg).

REFERENCES

1. *Fairlamb*, A.H. Novel biochemical pathways in parasitic protozoa. Parasitology 99S:93–112, 1989.
2. Fairlamb, A.H., Cerami, A. Metabolism and functions of trypanothione in the Kinetoplastida. Annu. Rev. Microbiol. 46:695–729, 1992.
3. Schirmer, R.H., Müller, J.G., Krauth-Siegel, R.L. Inhibitors of disulfide reductases as chemotherapeutic agents. Drug design against trypanosomiasis and malaria. Angew. Chemie Int. Ed. Engl. 34:141–154, 1995.
4. Fairlamb, A.H., Blackburn, P., Ulrich, P., Chait, B.T., Cerami, A. Trypanothione: A novel bis(glutathionyl)spermidine cofactor for glutathione reductase in trypanosomatids. Science 227:1485–1487, 1985.
5. Krauth-Siegel, R.L., Enders, B., Henderson, G.B., Fairlamb, A.H., Schirmer, R.H. Trypanothione reductase from *Trypanosoma cruzi*. Purification and characterization of the crystalline enzyme. Eur. J. Biochem. 164:123–128, 1987.
6. Sullivan, F.X., Walsh, C.T. Cloning, sequencing, overproduction and purification of trypanothione reductase from *Trypanosoma cruzi*. Mol. Biochem. Parasitol. 44:145–147, 1991.
7. Kuriyan, J., Kong, X.P., Krishna, T.S.R., Sweet, R.M., Murgolo, N.J., Field, H., Cerami, A., Henderson, G.B. X-ray structure of trypanothione reductase from *Crithidia fasciculata* at 2.4 Å resolution. Proc. Natl. Acad. Sci. U.S.A. 88:8764–8768, 1991.
8. Hunter, W.N., Bailey, S., Habash, J., Harrop, S.J., Helliwell, J.R., Aboagye-Kwarteng, T., Smith, K., Fairlamb, A.H. Active site of trypanothione reductase. A target for rational drug design. J. Mol. Biol. 227:322–333, 1992.
9. Lantwin, C.B., Schlichting, I., Kabsch, W., Pai, E.F., Krauth-Siegel, R.L. The structure of *Trypanosoma cruzi* trypanothione reductase in the oxidized and NADPH reduced state. Proteins 18:161–173, 1994.
10. Williams, C.H., Jr. Lipoamide dehydrogenase, glutathione reductase, thioredoxin reductase, and mercuric ion reductase—a family of flavoenzyme transhydrogenases. In: "Chemistry and Biochemistry of Flavoenzymes." Vol. III. Müller, F. (ed.). Boca Raton, FL: CRC Press, 1992:121–211.
11. Krauth-Siegel, R.L., Schöneck, R. Trypanothione reductase and lipoamide dehydrogenase as targets for a structure-based drug design. FASEB J. 9:1138–1146, 1995.
12. Jockers-Scherübl, M.C., Schirmer, R.H., Krauth-Siegel, R.L. Trypanothione reductase from *Trypanosoma cruzi*. Catalytic properties of the enzyme and inhibition studies with trypanocidal compounds. Eur. J. Biochem. 180:267–272, 1989.
13. Henderson, G.B., Ulrich, P., Fairlamb, A.H., Rosenberg, J., Pereira, M., Sela, M., Cerami, A. 'Subversive' substrates for the enzyme trypanothione disulfide reductase: Alternative approach to chemotherapy of Chagas' disease. Proc. Natl. Acad. Sci. U.S.A. 85:5374–5378, 1988.
14. Cênas, N., Bironaite, D., Dickancaite, E., Anusevicius, Z., Sarlauskas, J., Blanchard, J.S. Chinifur, a selective inhibitor and "subversive substrate" for *Trypanosoma congolense* trypanothione reductase. Biochem. Biophys. Res. Commun. 204:224–229, 1994.
15. Krauth-Siegel, R.L., Lohrer, H., Bücheler, U.S., Schirmer, R.H. The antioxidant enzymes glutathione reductase and trypanothione reductase as drug targets. In: "Biochemical Protozoology." Coombs, G., North, M. (eds.). London: Taylor & Francis, 1991:493–506.
16. Benson, T.J., McKie, J.H., Garforth, J., Borges, A., Fairlamb, A.H., Douglas, K.T. Rationally designed selective inhibitors of trypanothione reductase. Phenothiazines and related tricyclics as lead structures. Biochem. J. 286:9–11, 1992.
17. Hammond, D.J., Cover, B., Gutteridge, W.E. A novel series of chemical structures active in vitro against the trypomastigote form of *Trypanosoma cruzi*. Trans. R. Soc. Trop. Med. Hyg. 78:91–95, 1984.
18. Krauth-Siegel, R.L., Sticherling, C., Jöst, I., Walsh, C.T., Pai, E.F., Kabsch, W., Lantwin, C.B. Crystallization and preliminary crystallographic analysis of trypanothione reductase from *Trypanosoma cruzi*, the causative agent of Chagas' disease. FEBS Lett. 317:105–108, 1993.
19. Kabsch, W. Automatic indexing of rotation diffraction patterns. J. Appl. Crystallogr. 21:67–71, 1988.
20. Kabsch, W. Automatic processing of rotation diffraction data from crystals of initially unknown symmetry and cell constants. J. Appl. Crystallogr. 26:795–800, 1993.
21. Brünger, A.T. X-PLOR (Version 3. 1), Yale University, New Haven, 1993.
22. Courseille, C., Busetta, B., Hospital, M. Structure cristalline et moléculaire de la quinacrine. Acta Crystallogr. B29:2349–2355, 1973.
23. Jones, T.A. A graphics model building and refinement system for macromolecules. J. Appl. Crystallogr. 11:268–272, 1978.
24. Read, R. Improved Fourier coefficients for maps using phases from partial structures with errors. Acta Crystallogr. A42:140–149, 1986.
25. Sullivan, F.X., Sobolov, S.B., Bradley, M., Walsh, C.T. Mutational analysis of parasite trypanothione reductase: Acquisition of glutathione reductase activity in a triple mutant. Biochemistry 19:2761–2767, 1991.
26. Bailey, S., Smith, K., Fairlamb, A.H., Hunter, W.N. Substrate interactions between trypanothione reductase and N^1-glutathionylspermidine disulphide at 0.28-nm resolution. Eur. J. Biochem. 213:67–75, 1993.
27. Verschueren, K.H.G., Seljeé, F., Rozeboom, H.J., Kalk, K.H., Dijkstra, B.W. Crystallographic analysis of the catalytic mechanism of haloalkane dehalogenase. Nature 363:693–698, 1993.
28. Birktoft, J.J., Blow, D.M. Structure of crystalline α-chymotrypsin. J. Mol. Biol. 68:187–240, 1972.
29. Schulz, G.E., Schirmer, R.H. "Principles of Protein Structure." New York: Springer-Verlag, 1979.
30. Gregoret, L.M., Rader, S.D., Fletterick, R.J., Cohen, F.E. Hydrogen bonds involving sulfur atoms in proteins. Proteins 9:99–107, 1991.
31. Schönleben-Janas, A., Kirsch, P., Mittl, P., Schirmer, R.H., Krauth-Siegel, R.L., submitted.
32. McGrath, M.E., Eakin, A.E., Engel, J.C., McKerrow, J.H., Craik, C.S., Fletterick, R.J. The crystal structure of cruzain: A therapeutic target for Chagas' disease. J. Mol. Biol. 247:251–259, 1995.